Nitric Oxide–Induced Apoptosis in Lymphoblastoid and Fibroblast Cells Dependent on the Phosphorylation and Activation of p53

Laura M. McLaughlin and Bruce Demple

Department of Genetics and Complex Diseases, Harvard School of Public Health, Boston, Massachusetts

Abstract

When nitric oxide (NO) is produced at micromolar concentrations, as during inflammation, exposure to surrounding cells is potentially cytotoxic. The NO-dependent signaling pathways that initiate cell death are thought to involve the tumor suppressor protein p53, but the degree to which this factor contributes to NO-induced cell death is less clear. Various reports either confirm or negate a role for p53 depending on the cell type and NO donor used. In this study, we have used several pairs of cell lines whose only differences are the presence or absence of p53, and we have treated these cell lines with the same NO donor, spermineNONOate (SPER/NO). Treatment with SPER/NO induced such apoptotic markers as DNA fragmentation, nuclear condensation, poly-(ADP-ribose) polymerase cleavage, cytochrome *c* release, and Annexin V staining. p53 was required for at least 50% of SPER/NO-induced apoptotic cell death in human lymphoblastoid cells and for almost all in primary and E1A-tranformed mouse embryonic fibroblasts, which highlights the possible importance of DNA damage for apoptotic signaling in fibroblasts. In contrast, p53 did not play a significant role in NO-induced necrosis. NO treatment also induced the phosphorylation of p53 at Ser^{15}; pretreatment with phosphoinositide-3 kinase (PI3K) family inhibitors, wortmannin, LY294002, and caffeine, blocked such phosphorylation, but the p38 mitogen-activated protein kinase inhibitor, SB203580, did not. Pretreatment with the PI3K family inhibitors also led to a switch from NO-induced apoptosis to necrosis, which implicates a PI3K-related kinase such as ataxia telangiectasia mutated (ATM) or ATR (ATM and Rad3 related) in p53-dependent NO-induced apoptosis. (Cancer Res 2005; 65(14): 6097-104)

Introduction

Nitric oxide (NO) is a free radical whose stability depends on both its own rate of production and the surrounding levels of oxygen and other reactive oxygen species (1). Although NO is often produced at nanomolar concentrations as a signaling molecule, NO has been documented at micromolar levels when produced by immune cells during an oxidative burst (2) or during ischemia-reperfusion (3). NO can nitrosylate metal centers in proteins directly, autoxidize to N_2O_3, or react with superoxide anion to form peroxynitrite (4). The oxidation products may then react with proteins, lipids, and DNA to cause broad cellular damage (5–7). Macrophage-derived NO was shown to cause DNA damage in neighboring cells (8), and such genotoxicity may be a link between chronic inflammatory diseases and increased risk of cancer (9).

Requests for reprints: Bruce Demple, Harvard School of Public Health, Room 509, Building 1, 665 Huntington Avenue, Boston, MA 02115-6021. Phone: 617-432-3462; Fax: 617-432-0377; E-mail: bdemple@hsph.harvard.edu.

High fluxes of NO have been shown to induce markers of apoptotic cell death (10, 11). Apoptosis is often characterized by mitochondrial permeability transition and the release of proapoptotic factors, resulting in the proteolytic activation of caspases (12). These proteases then cleave cellular proteins, including poly(ADP-ribose) polymerase (PARP), resulting in the morphologic characteristics of apoptosis: DNA fragmentation, nuclear condensation, and cell shrinkage. Whereas NO treatment can inactivate caspases (13, 14), NO and its oxidation products also can inhibit electron transport proteins, thereby decreasing the transmembrane potential and oxidative phosphorylation in the mitochondria (15). Apoptosis is an energy-dependent process, and it was shown that NO could also induce a necrotic type of cell death, often characterized by loss of plasma membrane integrity and cellular swelling (16, 17). A major goal of our work was to characterize the cytotoxicity of NO in mammalian cells and determine how this cytotoxicity is regulated.

A key regulator of apoptosis is the tumor suppressor protein p53, a transcription factor that is capable of activating genes involved in DNA repair, growth arrest, and apoptosis. Both pure NO gas and 3-morpholinosydnonimine (SIN-1, which produces peroxynitrite by releasing both NO and O_2^-) can induce mutation in lymphoblastoid cells, which is increased in p53-deficient cells (18, 19). Treatment with the NO donor *S*-nitrosoglutathione (an NO donor that participates in nitrosation reactions) can induce apoptosis that is partially dependent on p53 (20), but a separate report from that group also showed that the monocytic cell line U937, which lacks p53, remains highly susceptible to *S*-nitrosoglutathione–induced apoptosis (21, 22). Primary cells derived from $p53^{-/-}$ mice also show varying sensitivity toward NO, with *S*-nitroso-*N*-acetyl penicillamine–induced apoptosis requiring p53 in thymocytes (23) but not in vascular smooth muscle cells (24). Wogan and coworkers showed that treatment with NO gas induces flipping of phosphatidylserine to the outer leaflet of the plasma membrane, another early hallmark of apoptosis, as well as mitochondrial membrane depolarization and permeability transition (18, 25). Whereas the effect of NO on the plasma membrane was dependent on p53, that of the mitochondrial membrane was not necessarily dependent on this factor.

Additionally, phosphorylation of p53 at the NH_2 terminus is critical for NO-mediated nuclear retention and activation of p53 (26, 27). Various kinases have been implicated in NO-induced p53 phosphorylation at Ser^{15}, including p38 mitogen-activated protein kinase (28), c-Jun NH_2-terminal kinase 1 and/or 2 (29), and the phosphoinositide 3-kinase (PI3K)–related kinases, ataxia telangiectasia mutated (ATM) and ATM and Rad3 related (ATR; refs. 27, 30). Again, the range of kinases implicated here most likely is due to the fact that different NO donors were used to treat different cell types in each of these studies. To address this problem, we have used spermineNONOate (SPER/NO), a member of the diazeniumdiolate family of NO donor compounds that release two molecules

of NO per donor molecule at a steady and reproducible rate (31). We used this NO donor to characterize NO-induced cytotoxicity in the following three cell lines: the lymphoblastoid cell line, TK6, primary murine embryonic fibroblasts (MEF), and E1A-transformed MEF cells. By comparing the amount and type of NO-induced cell death in these cell lines with that of their p53-deficient/null counterparts (otherwise genetically identical), we were able to clearly show the degree to which p53 plays a role in NO-induced apoptosis and necrosis. We were also able to use this system to explore further the NO-induced signaling mechanism that leads to the phosphorylation and activation of p53, ultimately causing NO-induced apoptosis.

Materials and Methods

Materials. SPER/NO [(*z*)-1-{*N*-[3-Aminopropyl]-*N*-[4-(3-aminopropylammonio)butyl]-amino}-diazen-1-ium-1,2-diolate] was purchased from Alexis Biochemicals (San Diego, CA). The fluorescent dyes, propidium iodide (PI), Hoechst No. 33258, and anti-β-actin antibody were from Sigma Chemical Co. (St. Louis, MO). Anti-PARP mouse monoclonal IgG1 (clone C-2-10) was from Zymed (South San Francisco, CA). Anti-cytochrome *c* mouse monoclonal IgG2b (clone 7H8.2C12) and the Annexin V/FITC staining kit were from BD PharMingen (San Diego, CA). Anti-p53 mouse monoclonal $IgG2_a$ (clone DO-1) and goat-anti-mouse and rabbit IgG linked to horseradish peroxidase were from Santa Cruz Biotechnology (Santa Cruz, CA). Anti-$p21^{WAF1}$ IgG1 (clone EA10) and anti-PUMA polyclonal antibody (rabbit) were from Oncogene (San Diego, CA). Anti-p53ser15-P and anti-Chk1ser345-P polyclonal antibodies were from Cell Signaling Technology (Beverly, MA). Enhanced chemiluminescence and chemifluorescence detection kits were from Amersham Biosciences (Piscataway, NJ).

Tissue culture. The lymphoblastoid cell lines, TK6, TK6-E6-5E, and TK6-E6-20C were gifts from Dr. John B. Little and were grown in RPMI 1640 (Mediatech, Herndon, VA) supplemented with 10% horse serum (Hyclone, Logan, UT), 50 IU/mL penicillin, 50 μg/mL streptomycin, 2 mmol/L glutamine (Life Technologies, New York, NY). These cell lines were grown at 37°C in 5% CO_2 inside a humidified incubator, and the cultures were kept at 1×10^4 to 4×10^5 cells/mL. Primary and E1A-transformed MEF cells were generous gifts from Dr. Tyler Jacks and Kenneth P. Olive (Department of Biology at The Massachusetts Institute of Technology) and were grown at 37°C in 10% CO_2, and cultures were kept between 10% and 90% confluency (32).

SpermineNONOate treatment. Cells were always treated for 1 hour at 37°C with either fresh SPER/NO or its stable decay products; the cells were then washed once with PBS before replacing the medium. Fresh SPER/NO solutions in medium were always made immediately before addition to the cells, whereas solutions of the stable decay products of SPER/NO were prepared at least 2 days before treatment and incubated at 37°C until beginning the cell treatment. The lymphoblastoid (suspension) cell lines were treated at 1×10^6 to 2×10^6 cells/mL, and after washing with PBS, diluted into fresh medium at 3×10^5 cells/mL. All MEF cells were treated at 70% confluency in either 60- or 100-mm plates. The decay half-life of SPER/NO under these conditions was estimated to be ~3 hours. We also measured the concentration of NO in cellular medium during the 1-hour treatment using an ISO-NO MARK II–isolated NO meter (World Precision Instruments, Sarasota, FL). The steady-state concentration of NO generated by 2 and 4 mmol/L SPER/NO rapidly reached, respectively, 7.7 ± 0.6 and 9.8 ± 1.3 μmol/L within the first 5 minutes and gradually rose to 11 ± 1.8 and 14 ± 0.2 μmol/L NO.

Cell staining and analysis. To detect apoptosis, cells were fixed in 70% ethanol overnight at 4°C and were stained with the DNA intercalating dye PI (50 μg/mL) in PBS containing 50 μg/mL RNase A. Cells with sub-G_1 DNA content (fragmented DNA and/or condensed chromatin) were scored as apoptotic. To characterize nuclear morphology, cells were stained with Hoechst No. 33258 (10 μg/mL in PBS containing 50 μg/mL RNase A) or the above PI solution, and then viewed by fluorescence microscopy (at least 300 cells were counted per sample). To differentiate between early apoptosis and late apoptosis/necrosis, cells were harvested various times after the SPER/NO treatment and immediately stained with Annexin V/FITC and PI according to the protocol provided by the manufacturer. The harvest and staining took ~1 hour, and then stained cells were immediately analyzed by flow cytometry. In all flow cytometry experiments, 5×10^3 to 1×10^4 events were recorded per sample.

Immunoblotting analysis. To make whole cell protein extracts, at least 1×10^6 cells (suspended and adherent) were harvested per sample, snap frozen for storage, and resuspended in cold cell lysis buffer [50 mmol/L HEPES (pH 7.4), 150 mmol/L NaCl, 1% NP40, 0.5% Na-deoxycholate, 0.1% SDS, 1 mmol/L DTT, also containing 100-fold diluted protease inhibitor cocktail for use with mammalian cell and tissue extracts from Sigma Chemical (4-(2-aminoethyl)benzenesulfonyl fluoride, pepstatin A, E-64, leupeptin, and aprotinin)]. After shearing the DNA, the extracts were centrifuged at 18,000 × *g* for 20 minutes (all done at 4°C), and the supernatant was retained. To separate cytosolic proteins from mitochondrial proteins, at least 5×10^6 cells were first incubated in "sucrose buffer" [250 mmol/L sucrose, 20 mmol/L HEPES, 10 mmol/L KCl, 1.5 mmol/L $MgCl_2$, 1 mmol/L EDTA, 1 mmol/L DTT (pH 7.4), and protease inhibitor cocktail as above] containing 0.1 mg/mL of digitonin for 3 minutes at 37°C to solubilize the plasma membrane and then centrifuged at 12,000 × *g* for 5 minutes at 4°C (33). The supernatant was removed and diluted with a 50% volume of cell lysis buffer ("cytosolic" fraction). The pellet (containing intact mitochondria and nuclei) was extracted using 1:1 mixture of sucrose and cell lysis buffers following the above protocol for the whole cell protein

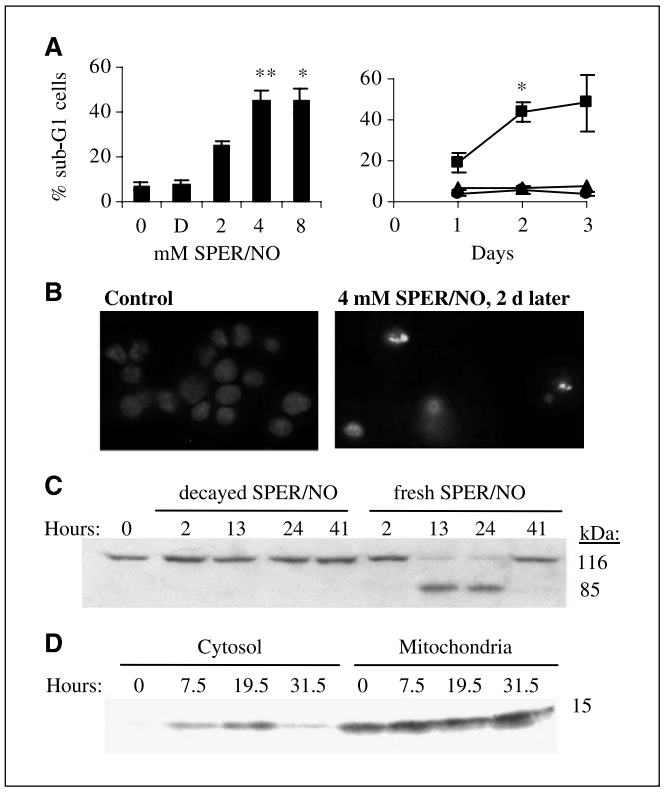

Figure 1. SPER/NO induces markers of apoptotic death in TK6 cells. *A,* TK6 cells were challenged for 1 hour with 0 mol/L (●), 4 mmol/L (■), decayed 4 mmol/L (▲) SPER/NO or at otherwise indicated concentrations (*D* = the stable decay products of SPER/NO) and analyzed by PI staining and flow cytometry 2 days later or at the indicated times. **, $P < 0.0005$; *, $P < 0.05$ compared with control. *B,* TK6 cells were challenged with 0 or 4 mmol/L SPER/NO for 1 hour. Nuclear condensation was detected 2 days after the challenge by Hoechst staining and fluorescence microscopy. *C* and *D,* TK6 cells were challenged for 1 hour with either 4 mmol/L fresh or decayed SPER/NO. PARP cleavage (*C*) and cytochrome *c* release into the cytosol (*D*) were measured by immunoblotting: 50 μg protein per well (*C*) and 20 μg protein per well (*D*).

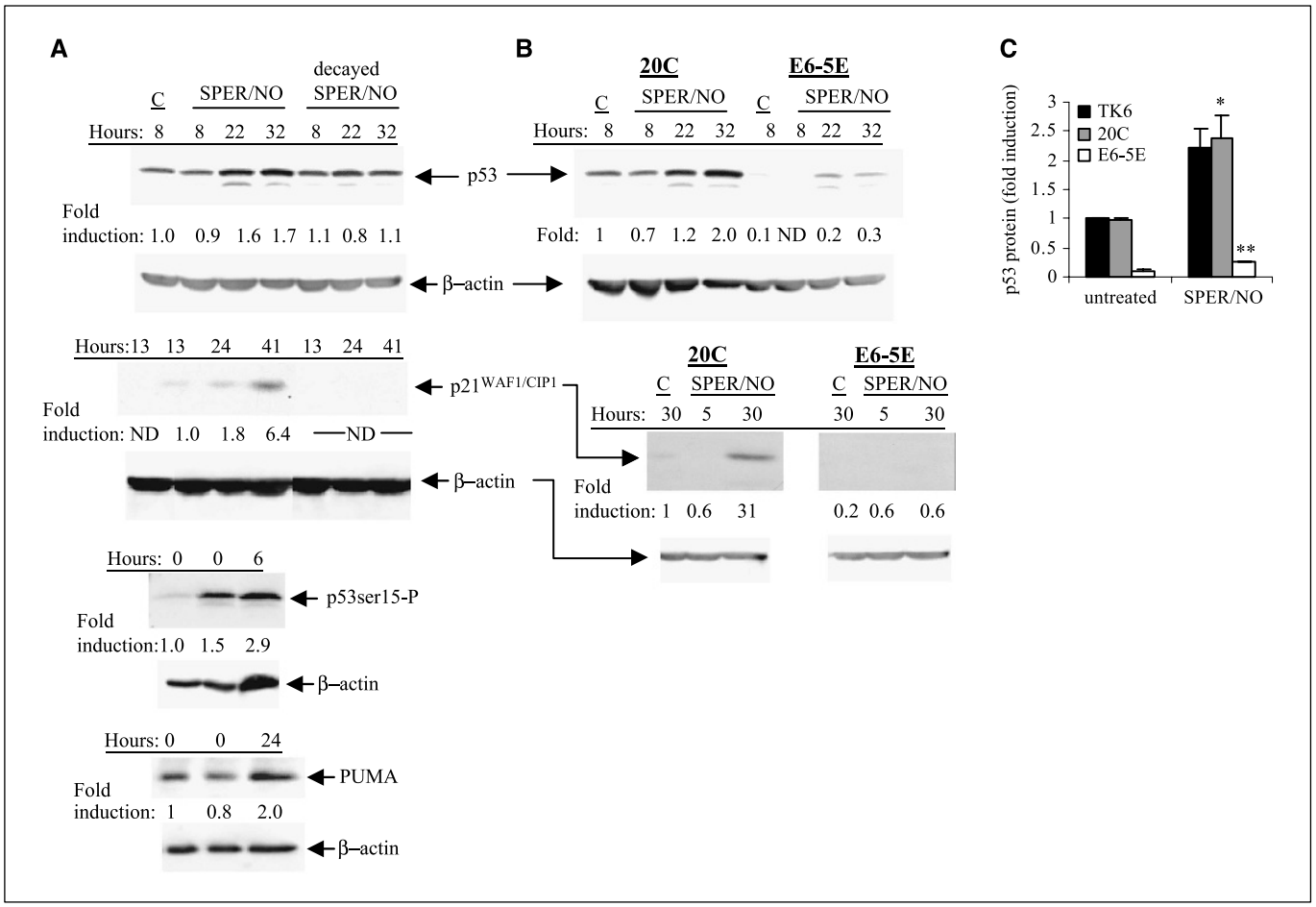

Figure 2. SPER/NO induces transcriptionally active p53 in TK6 cell lines. *A,* TK6 cells challenged 1 hour with fresh or decayed 4 mmol/L SPER/NO were incubated for various times and analyzed for p53, p53ser15-P, $p21^{WAF1/Cip1}$, PUMA ($n = 2$), and β-actin (loading control) proteins by immunoblotting (50 μg protein per well). *C,* control; *ND,* not detected. *B,* TK6-E6-5E (E6 transformed, p53 deficient) and 20C (vector control, expressing p53) cells were challenged for 1 hour with fresh 4 mmol/L SPER/NO; p53, $p21^{WAF1/Cip1}$ ($n = 2$), and β-actin protein levels detected by immunoblotting (50 μg protein per well). *C,* the mean induction of p53 protein levels in TK6, TK6-20C, and TK6-E6-5E, 1 day after treatment with 4 mmol/L SPER/NO for 1 hour. *, $P < 0.05$ when comparing 4 mmol/L SPER/NO-treated TK6-20C cells with untreated cells; **, $P < 0.05$ when comparing 4 mmol/L SPER/NO-treated TK6-E6-5E and TK6-20C cells.

extracts ("mitochondrial" fraction). Proteins were separated by SDS-PAGE (12% polyacrylamide resolving gels when detecting cytochrome *c* and 10% for all other proteins) and transferred to nitrocellulose membranes, which were blocked with 5% powdered milk in PBS containing 0.05% Tween 20 for 25 minutes at room temperature with gentle shaking. Membranes were incubated with the primary antibody reactive against p53 (1:5,000, 45 minutes at room temperature); p53ser15-P, Chk1ser345-P, and $p21^{WAF1/Cip1}$ (1:1,000, overnight at 4°C); p53-up-regulated modulator of apoptosis (PUMA, 1:200, 1 hour at room temperature); β-actin (1:4,000, 1 hour at room temperature); cytochrome *c* (1:100, 1 hour at room temperature); and PARP (1:500, overnight at 4°C). Then, after incubating with the appropriate species-specific IgG conjugates, the membranes were exposed to chemiluminescence or chemifluorescence reagents. The resulting chemiluminescence was detected by exposure to Kodak BioMax film (New Haven, CT), whereas the chemifluorescence signal was detected using the Storm 840 phophorimager (Molecular Dynamics, Sunnyvale, CA). Scion Image 4.0.2 software was used to quantify band intensities from images on film, and Imagequant software was used to quantify band intensities detected by phosphorimager. All blots shown are representative of three experiments unless otherwise indicated.

Statistics. The results presented are the mean of at least three independent experiments, unless stated otherwise, and the error bars correspond to the SEs of the mean. All *P* values correspond to two-sample *t* tests assuming unequal variances, unless indicated otherwise.

Results

Nitric oxide induces apoptosis in nontransformed human cells. To expose cells to NO, incubations were carried out for 1 hour with SPER/NO, which releases two molecules of NO during the decay of each donor molecule. To detect cell death in the human lymphoblastoid cell line TK6, sub-G_1 DNA content was measured by PI staining and flow cytometry analysis. SPER/NO induced a dose-dependent increase in the sub-G_1 population in TK6 cells, which peaked 2 days after the treatment (Fig. 1*A*). The presence of condensed and picnotic nuclei was also detected microscopically in the NO-treated cells (Fig. 1*B*). To define the NO-induced apoptotic pathway more precisely, we examined the kinetics of common molecular markers of apoptosis, including the cleavage of the caspase substrate PARP into the 85-kDa cleavage product (Fig. 1*C*), and the release of cytochrome *c* into the cytosol (Fig. 1*D*). SPER/NO treatment induced both of these markers, which was consistent with the activation of an apoptotic signaling pathway that requires the involvement of mitochondria to activate caspases and mediate the death of the cell. Importantly, SPER/NO that had been allowed to decompose fully to its stable decay products was not able to induce any of the markers of apoptotic cell death measured here (Fig. 1*A* and *D*). Thus, the effects

observed depend on NO rather than some other stable decay product.

Nitric oxide induces transcriptionally active p53. Next, we measured NO-dependent induction of p53 in the lymphoblastoid cells. p53 protein levels were induced 1 day after treatment with SPER/NO (Fig. 2*A* and *C*); however, p53 induction in NO-treated TK6 cells occurred after that of cytochrome *c* release (Fig. 1*D*) and PARP cleavage (Fig. 1*C*), which was detectable as early as 6 hours (data not shown). Thus, the role of p53 in NO-induced cell death remained uncertain.

The levels of p53 protein are kept low in nonstressed cells by Mdm-2, which binds to the p53 NH_2 terminus and regulates its degradation and export from the nucleus (34). During genotoxic stress, residues in the NH_2 terminus of p53 become phosphorylated, including Ser^{15}, which correlates with decreased binding of Mdm-2 to p53 (35). Alternatively, p53 phosphorylation at Ser^{15} was shown sufficient to block p53 nuclear export irrespective of Mdm-2 (36). SPER/NO did significantly induce phosphorylation of p53 at Ser^{15} in TK6 cells (Fig. 2*A*). Because this phosphorylation preceded the induction of the p53 transcriptional targets, $p21^{WAF1/Cip1}$ (Fig. 2*A*), and the apoptotic markers measured in Fig. 1, these data suggest that NO can rapidly activate the transcriptional activity of p53 in TK6 cells, and a role for p53 could not be ruled out. In accordance with these results and with a potential role for p53 in NO-induced apoptosis, NO treatment caused a slight increase in the proapoptotic p53 transcriptional target PUMA (Fig. 2*A*; ref. 37). This modest increase in PUMA in response to NO is consistent with a recently published study (25).

Nitric oxide induces p53-dependent apoptosis in lymphoblastoid cells and murine embryonic fibroblasts. To gauge the actual contribution of p53 in NO-induced cell death, we used two cell lines derived from TK6 that were stably transfected with a plasmid expressing HPV16 E6 (TK6-E6-5E) or the empty vector (TK6-20C). The E6 protein mediates p53 degradation by the proteasome (38). Whereas the NO treatment did induce p53 and $p21^{WAF1/Cip1}$ protein levels in the vector control cell line (TK6-20C), p53 induction was substantially lower (10% of TK6-20C) and $p21^{WAF1/Cip1}$ induction was not detectable in the corresponding E6-expressing cell line (TK6-E6-5E; Fig. 2*B* and *C*). Thus, the expression of E6 produced a p53 deficiency that showed the p53 dependence of $p21^{WAF1/Cip1}$ induction by NO.

Figure 3 shows that the p53-deficienct cell line, TK6-E6-5E, was significantly more resistant to NO-induced apoptosis, including PARP cleavage and cytochrome *c* release, than was the vector control cell line, TK6-20C. After the baseline had been subtracted out, 2 and 4 mmol/L SPER/NO-induced DNA fragmentation was significantly dependent on p53 (Fig. 3*B*). However, there was little or no difference between the two cell lines at later times (Fig. 3*A, C*, and *D*). These observations suggest that NO induces both p53-dependent and -independent pathways of cell death. However, the E6-expressing cell line retains a low residual level of p53 (Fig. 2*B*) that could contribute to NO-induced cell death. Therefore, additional experiments were carried out in cells devoid of p53.

NO-induced cell death was measured in MEF cells derived from $p53^{+/-}$ or $p53^{-/-}$ mice. The $p53^{-/-}$ MEF cells were significantly more resistant to NO-induced nuclear condensation than were the $p53^{+/-}$ cells (Fig. 4*A*). The interpretation of these results was complicated by the rather low level of apoptosis induced by NO in the $p53^{+/-}$ cells. An alternative was provided by E1A-transformed MEF cells, which are much more sensitive to genotoxic stresses

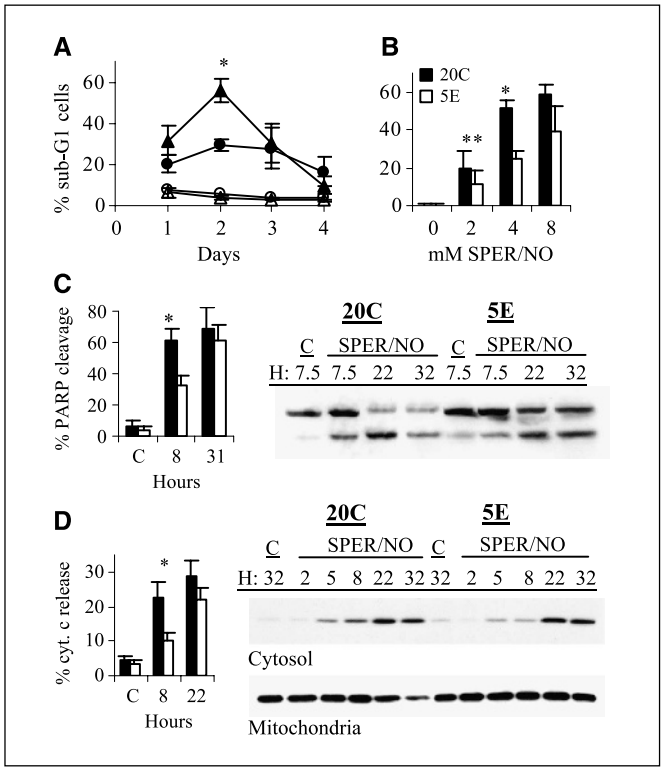

Figure 3. SPER/NO induces apoptosis in both p53-proficient and -deficient cells. *A* and *B,* TK6-E6-5E (E6 transformed, p53 deficient, ● and ○) and 20C (vector control, expressing p53, ▲ and △) cells were challenged for 1 hour with 0 (○ and △) or 4 mmol/L (● and ▲) SPER/NO (*A*) or other indicated concentrations (*B*). PI staining and flow cytometry were done 2 days later (*B*) or as indicated (*A*). *, $P < 0.005$ and **, $P < 0.05$ (in a paired sample *t* test) comparing 20C and 5E cells 2 days after the challenge. *C* and *D,* TK6-E6-5E (*empty columns*) and 20C (*filled columns*) cells were challenged with 4 mmol/L SPER/NO (*C,* untreated control) for 1 hour and incubated as indicated (*H,* hours). PARP cleavage (*C*) and cytochrome *c* release (*D*: *top*, cytosolic fraction; *bottom*, mitochondrial fraction) were measured by immunoblotting: 50 μg protein per well (*C*) and 20 μg protein per well (*D*). *, $P < 0.05$ comparing 20C and 5E cells, 8 hours after 4 mmol/L SPER/NO challenge.

(32). We characterized NO-induced cell death in E1A wild type (WT) and $p53^{-/-}$ MEF cells by staining with Annexin V/FITC and PI and then analyzing them by flow cytometry (Fig. 4*B, C*, and *D*). Annexin V protein specifically binds phosphatidylserine, a phospholipid that is normally present only on the inner leaflet of the plasma membrane but which is flipped to the outer leaflet during apoptotic signaling. However, only cells that have lost membrane integrity, such as those undergoing necrosis or in the late stages of apoptosis, may be stained with PI (39). Figure 4*B* shows the kinetics of PI and Annexin V staining for both E1A-WT and E1A-$p53^{-/-}$ MEFs after a 1-hour treatment with 2 mmol/L SPER/NO. For the WT cells, the Annexin $V/FITC^+/PI^-$ population reached its peak before that of the Annexin $V/FITC^+/PI^+$, which indicates that the NO treatment did induce apoptosis in the $p53^{+/+}$ cells. However, the large peak in Annexin $V/FITC^+/PI^+$ at 6 hours suggests that some cells were undergoing necrosis. For the $p53^{-/-}$cells, the peak in the Annexin $V/FITC^+/PI^+$ population was not preceded by a peak in the Annexin $V/FITC^+/PI^-$ population, which indicates that the NO treatment induced only necrosis in the absence of p53. Again, there seemed at least two different pathways of NO-induced cell death, in which NO-induced apoptosis was completely dependent on p53 (Fig. 4*B-C*).

Comparison of the WT and p53$^{-/-}$ E1A-transformed MEF cells indicates that NO-induced necrosis did not require p53.

Inhibition of kinase-signaling upstream of p53 shifts spermineNONOate-induced cell death toward necrosis. To elucidate the mechanism by which NO induces p53-dependent cell death, the contribution of kinases upstream of p53 to NO-induced cell death was explored. We chose Ser^{15} phosphorylation as a marker for p53 NH_2 terminus phosphorylation; this residue has been implicated in NO-mediated p53-regulation (26, 27, 30), and changing Ser^{15} to alanine diminished radiation-induced apoptosis in mouse thymocytes (40). Figure 5*A* and *C* shows that whereas the p38 mitogen-activated protein kinase inhibitor SB203580 had no detectable effect on SPER/NO-induced p53ser15 phosphorylation, two inhibitors of the PI3K family, wortmannin and LY294002, and the ATM/ATR inhibitor, caffeine, reduced such phosphorylation. It is also important to note that, although wortmannin alone caused a low amount of cell death, treatment with caffeine, LY294002, or SB203580 alone did not cause detectable toxicity (data not shown). Next, the contribution of PI3K family members to NO-induced cell death was assessed. To control for variation in the absolute amount of cell death induced by SPER/NO in different experiments, the data in Fig. 5*D* are presented as the ratio of the percentage of cells in the Annexin V/FITC$^+$/PI$^-$ population to that of the Annexin V/FITC$^+$/PI$^+$ population. Thus, a value of >1 indicates that more cells were undergoing apoptosis than necrosis, while a value of <1 indicates that more cells were undergoing necrosis. Both wortmannin and LY294002 shifted NO-induced apoptosis toward necrosis in WT cells but not in p53$^{-/-}$ cells. Thus, the target of these inhibitors likely acts in the same pathway as does p53 in response to NO. In agreement with these observations, the PI3K-related kinase family members ATM and ATR are implicated in NO-induced p53ser15 phosphorylation (30). Specifically, ATR was shown to play a role in NO-induced nuclear localization of p53 (27). Likewise in our studies, NO treatment induced phosphorylation of the ATR substrate Chk1 (Ser^{345}), which was attenuated by the inhibitors wortmannin, LY294002, and caffeine (Fig. 5*A*).

Discussion

We have shown that the NO donor SPER/NO induces the hallmark features of apoptosis, including release of cytochrome *c* into the cytosol, cleavage of the caspase substrate PARP, and nuclear condensation. These observations are in agreement with a previous report where treatment with pure NO gas induced mitochondrial dysfunction and nuclear condensation in TK6 cells (41), as well as another report in which a general caspase inhibitor blocked apoptosis induced by *S*-nitrosoglutathione in murine macrophages (42). The fact that decayed SPER/NO failed to induce these apoptotic markers points to the specific role of NO. In addition, by comparing the ability of NO exposure to induce apoptosis in three different cell models, each a set differing only in the p53 status, we defined a role for this tumor suppressor protein in NO-induced apoptosis. Apoptosis induced by NO was significantly delayed in p53-deficient TK6 cells and absent from p53$^{-/-}$ primary and E1A-transformed MEF cells. However, the available data indicate that NO-induced necrosis does not require p53. Therefore, although NO clearly induces p53-dependent apoptosis, NO can induce other cell death signaling pathways that ultimately result in either apoptosis or necrosis.

Li et al. also implicated p53 in the apoptosis induced by exposure of TK6 cells to pure NO gas (comparable with the levels of NO used in the present study; ref. 18). This group showed that the NO induction of two common markers of apoptosis, phosphatidylserine flipping and DNA fragmentation, were significantly dependent on p53. However, NO-induced mitochondrial membrane depolarization was independent of p53. This group also showed conflicting results on the NO-induced release of proapoptotic factors from the

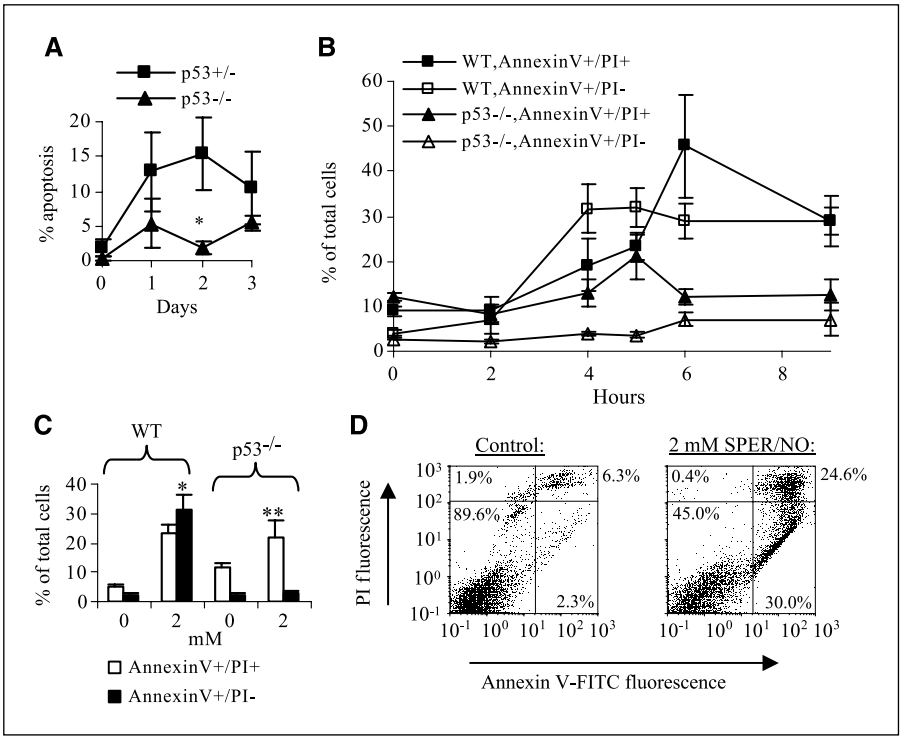

Figure 4. SPER/NO induces p53-dependent apoptosis in MEFs. *A,* primary p53$^{+/-}$ and p53$^{-/-}$ MEFs were challenged for 1 hour with 4 mmol/L SPER/NO. Apoptosis was measured by Hoechst staining and counting cells with condensed and picnotic nuclei by fluorescence microscopy. *, $P < 0.05$. *B* and *C,* WT and p53$^{-/-}$ E1A-MEF cells were challenged for 1 hour with 0 or 2 mmol/L SPER/NO and stained with Annexin V/FITC and PI 5 hours later (*C*) or at the indicated times (*B*). The Annexin V$^+$/PI$^-$ and Annexin V$^+$/PI$^+$ populations were measured by fluorescence-activated cell sorting. *, $P < 0.05$ comparing treated with nontreated cells; **, $P > 0.05$ comparing Annexin V$^+$/PI$^+$ in treated WT and p53$^{-/-}$ cells. *D,* representative flow cytometry results from at least three different experiments. *Bottom left quadrant,* PI$^-$ and Annexin V$^-$ (viable) cells; *bottom right quadrant,* PI$^-$ and Annexin V$^+$ (early apoptotic) cells; *top right quadrant,* PI$^+$ and Annexin V$^+$ (late apoptotic and necrotic) cells.

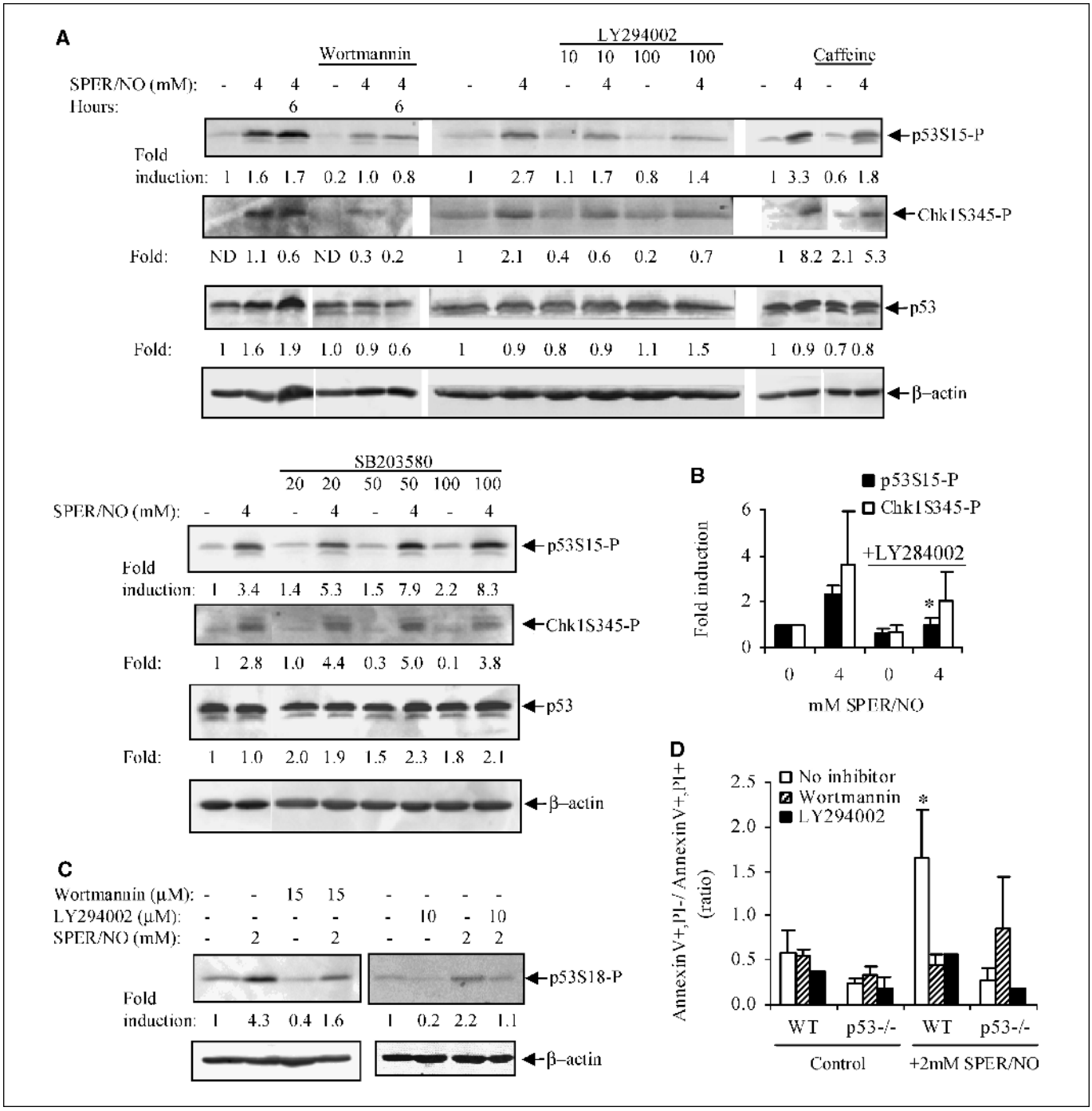

Figure 5. PI3K inhibitors reduce p53ser15 phosphorylation and shift SPER/NO-induced apoptosis to necrosis. *A,* TK6 cells were pretreated with wortmannin (15 μmol/L for 2 hours), LY294002 (10 or 100 μmol/L for 2 hours), caffeine (5 mmol/L for 2 hours), or SB203580 (20, 50, and 100 μmol/L for 30 minutes) and challenged 1 hour with 4 mmol/L SPER/NO. Samples were taken after the challenge at the times indicated. p53ser15 and Chk1ser345 phosphorylation, p53, and β-actin protein levels were detected by immunoblotting (50 protein μg per well). *B,* the mean levels of p53ser15 and Chk1ser345 phosphorylation (normalized to β-actin) are shown for TK6 cells pretreated with 0 or 100 μmol/L LY294002, immediately after the 1-hour treatment with 0 or 4 mmol/L SPER/NO. *, $P < 0.05$ when comparing 4 mmol/L SPER/NO-treated samples that were pretreated with 0 or 100 μmol/L LY294002. *C,* E1A-MEF cells pretreated for 2 hours with 15 μmol/L wortmannin or 10 μmol/L LY294002 and were challenged with 2 mmol/L SPER/NO for 1 hour. p53ser18 phosphorylation was detected by immunoblotting. Blots shown are representative of at least three (*A*) or two (*C*) experiments. *D,* E1A-MEFs, 5 hours after treatment with 0 or 2 mmol/L SPER/NO, were analyzed for the Annexin V^+/PI^- and Annexin V^+/PI^+ populations by Annexin V/FITC and PI staining and flow cytometry. The ratio of these two populations is shown. *, $P < 0.05$ when comparing non-pretreated/2 mmol/L SPER/NO-treated WT with $p53^{-/-}$ cells or pretreated/2 mmol/L SPER/NO-treated WT cells.

mitochondria; the mitochondrial loss of apoptosis inducing factor and endonuclease G was p53 dependent, but the release of cytochrome *c* and SMAC/DIABLO was p53 independent (18, 25). Our results in essentially the same lymphoblastoid cells showed that NO-induced cytochrome *c* release was considerably delayed in the absence of p53. The key difference between these sets of experiments lies in the method of p53 inactivation. In our experiments, p53 was functionally inactivated by expression of E6

protein, whereas in Li et al., TK6 cells were compared with WTK1 cells, which are closely related to TK6 but contain a mutation of the *p53* gene that substitutes methionine for isoleucine in codon 237 (43). The mutant p53 protein is highly expressed in WTK1 cells, but this mutation occurs in the p53 DNA binding domain, which suggests that the mutant protein cannot function adequately as a transcription factor. It also was shown that p53 can itself localize to the mitochondria to cause apoptosis, and that a transcriptionally inactive mutant of p53 (R175H) could still induce cell death when targeted to the mitochondria (44). In addition, p53 can interact directly with Bax to mediate lipid membrane permeability (45). Therefore, it is possible that this alternative activity of p53 can still be carried out by the p53 M237I mutant and that this activity reconciles the difference between the results of Li et al. and those we present here (18, 25).

Phosphorylation of the NH_2 terminus of p53 is a key mechanism by which the cell regulates p53 function. Several groups have implicated phosphorylation of the p53 NH_2 terminus as a critical event in NO-dependent induction of p53 protein and activity (30, 46). The p38 mitogen-activated protein kinase was shown to play a role in sodium nitroprusside-induced p53ser15 phosphorylation and cell death in primary rabbit articular chondrocytes (28). In contrast, in our experiments, p38 mitogen-activated protein kinase was not significantly involved in NO-induced p53ser15 phosphorylation in lymphoblastoid cells. Instead, our results implicate PI3K family members in NO-induced p53ser15 phosphorylation and p53-dependent apoptosis. Treatment with the PI3K inhibitors LY294002 or wortmannin shifted NO-induced apoptosis to necrosis only in cells with functional p53, highlighting the dependence of NO-induced apoptosis on p53 in these cells. Our finding that LY294002 shifts NO-induced apoptosis toward necrosis also was recently corroborated in primary murine astrocytes (47). Additionally, a mutant p53 protein, in which the phosphorylation sites in the NH_2 terminus were mutated to alanines (including Ser^{15}), was shown resistant to NO-induced nuclear retention (26). Overexpression of a "kinase-dead" mutant of ATR blocked NO-induced p53ser15 phosphorylation and nuclear retention, implicating this PI3K-related kinase in the response (27). Our results also show that inhibitors of the PI3K family, wortmannin and LY294002, and the ATM/ATR inhibitor caffeine, could attenuate but not fully block NO-induced p53ser15 phosphorylation in TK6 cells (Fig. 5*A*). Because c-Jun NH_2-terminal kinases 1 and 2 have also been implicated in NO-induced p53 phosphorylation, these kinases also could be responsible for the residual p53ser15 phosphorylation observed (29).

The role of p53 in apoptosis induced by NO indicates a significant level of DNA damage accompanying the exposure, although some recent work also suggests that disruption of nucleolar function activates p53 independently of DNA damage (48). In the absence of p53, a fail-safe mechanism exists such that cell death still can proceed, either in the form of apoptosis or necrosis. The mechanism by which NO leads to cell death in these cases is unclear. While it is possible that DNA damage is the origin of the p53-independent cell death signaling in cells exposed to NO, components of the mitochondria- and endoplasmic reticulum stress–signaling pathways should be investigated.

Acknowledgments

Received 11/29/2004; revised 4/7/2005; accepted 4/27/2005.

Grant support: NIH grant CA82737 and National Cancer Institute training grant T32-09078 (L.M. McLaughlin).

The costs of publication of this article were defrayed in part by the payment of page charges. This article must therefore be hereby marked *advertisement* in accordance with 18 U.S.C. Section 1734 solely to indicate this fact.

We thank Dr. Tyler Jacks and Kenneth P. Olive for providing us with the primary and E1A-transformed MEF cells; Dr. John B. Little for providing us with the TK6 cell lines used here; Amy Imrich, Yuhong Xiang, and colleagues for their technical support and expertise in fluorescence-activated cell sorting analysis; and Dr. Zhi-Min Yuan and our colleagues from the Demple Laboratory for advice on experiments and the article.

References

1. Beckman JS, Koppenol WH. Nitric oxide, superoxide, and peroxynitrite: the good, the bad, and ugly. Am J Physiol 1996;271:C1424–37.
2. Hibbs JB Jr, Taintor RR, Vavrin Z, Rachlin EM. Nitric oxide: a cytotoxic activated macrophage effector molecule. Biochem Biophys Res Commun 1988;157:87–94.
3. Zhang ZG, Chopp M, Bailey F, Malinski T. Nitric oxide changes in the rat brain after transient middle cerebral artery occlusion. J Neurol Sci 1995;128:22–7.
4. Espey MG, Miranda KM, Thomas DD, et al. A chemical perspective on the interplay between NO, reactive oxygen species, and reactive nitrogen oxide species. Ann N Y Acad Sci 2002;962:195–206.
5. Caulfield JL, Wishnok JS, Tannenbaum SR. Nitric oxide-induced deamination of cytosine and guanine in deoxynucleosides and oligonucleotides. J Biol Chem 1998;273:12689–95.
6. Szabo C, Ohshima H. DNA damage induced by peroxynitrite: subsequent biological effects. Nitric Oxide 1997;1:373–85.
7. Tamir S, Burney S, Tannenbaum SR. DNA damage by nitric oxide. Chem Res Toxicol 1996;9:821–7.
8. Watanabe N, Miura S, Zeki S, Ishii H. Hepatocellular oxidative DNA injury induced by macrophage-derived nitric oxide. Free Radic Biol Med 2001;30:1019–28.
9. Hussain SP, Hofseth LJ, Harris CC. Radical causes of cancer. Nat Rev Cancer 2003;3:276–85.
10. Albina JE, Cui S, Mateo RB, Reichner JS. Nitric oxide-mediated apoptosis in murine peritoneal macrophages. J Immunol 1993;150:5080–5.
11. Fehsel K, Kroncke KD, Meyer KL, Huber H, Wahn V, Kolb-Bachofen V. Nitric oxide induces apoptosis in mouse thymocytes. J Immunol 1995;155:2858–65.
12. Hengartner MO. The biochemistry of apoptosis. Nature 2000;407:770–6.
13. Mannick JB, Schonhoff C, Papeta N, et al. S-nitrosylation of mitochondrial caspases. J Cell Biol 2001;154:1111–6.
14. Rossig L, Fichtlscherer B, Breitschopf K, et al. Nitric oxide inhibits caspase-3 by S-nitrosation *in vivo*. J Biol Chem 1999;274:6823–6.
15. Poderoso JJ, Carreras MC, Lisdero C, Riobo N, Schopfer F, Boveris A. Nitric oxide inhibits electron transfer and increases superoxide radical production in rat heart mitochondria and submitochondrial particles. Arch Biochem Biophys 1996;328:85–92.
16. Leist M, Single B, Naumann H, et al. Inhibition of mitochondrial ATP generation by nitric oxide switches apoptosis to necrosis. Exp Cell Res 1999;249:396–403.
17. Nicotera P, Melino G. Regulation of the apoptosis-necrosis switch. Oncogene 2004;23:2757–65.
18. Li CQ, Trudel LJ, Wogan GN. Nitric oxide-induced genotoxicity, mitochondrial damage, and apoptosis in human lymphoblastoid cells expressing wild-type and mutant p53. Proc Natl Acad Sci U S A 2002;99:10364–9.
19. Li CQ, Trudel LJ, Wogan GN. Genotoxicity, mitochondrial damage, and apoptosis in human lymphoblastoid cells exposed to peroxynitrite generated from SIN-1. Chem Res Toxicol 2002;15:527–35.
20. Messmer UK, Ankarcrona M, Nicotera P, Brune B. p53 expression in nitric oxide-induced apoptosis. FEBS Lett 1994;355:23–6.
21. Brockhaus F, Brune B. U937 apoptotic cell death by nitric oxide: Bcl-2 downregulation and caspase activation. Exp Cell Res 1998;238:33–41.
22. Messmer UK, Brune B. Nitric oxide-induced apoptosis: p53-dependent and p53-independent signalling pathways. Biochem J 1996;319:299–305.
23. Gordon SA, Abou-Jaoude W, Hoffman RA, et al. Nitric oxide induces murine thymocyte apoptosis by oxidative injury and a p53-dependent mechanism. J Leukoc Biol 2001;70:87–95.
24. Kibbe MR, Li J, Nie S, et al. Potentiation of nitric oxide-induced apoptosis in p53−/− vascular smooth muscle cells. Am J Physiol Cell Physiol 2002;282:C625–34.
25. Li CQ, Robles AI, Hanigan CL, et al. Apoptotic signaling pathways induced by nitric oxide in human lymphoblastoid cells expressing wild-type or mutant p53. Cancer Res 2004;64:3022–9.
26. Schneiderhan N, Budde A, Zhang Y, Brune B. Nitric oxide induces phosphorylation of p53 and impairs nuclear export. Oncogene 2003;22:2857–68.
27. Wang X, Zalcenstein A, Oren M. Nitric oxide promotes p53 nuclear retention and sensitizes neuroblastoma cells to apoptosis by ionizing radiation. Cell Death Differ 2003;10:468–76.
28. Kim SJ, Hwang SG, Shin DY, Kang SS, Chun JS. p38 kinase regulates nitric oxide-induced apoptosis of articular chondrocytes by accumulating p53 via NFκ B-dependent transcription and stabilization by serine 15 phosphorylation. J Biol Chem 2002;277:33501–8.
29. Callsen D, Brune B. Role of mitogen-activated protein kinases in *S*-nitrosoglutathione-induced macrophage apoptosis. Biochemistry 1999;38:2279–86.

30. Hofseth LJ, Saito S, Hussain SP, et al. Nitric oxide-induced cellular stress and p53 activation in chronic inflammation. Proc Natl Acad Sci U S A 2003;100:143–8.
31. Fitzhugh AL, Keefer LK. Diazeniumdiolates: pro- and antioxidant applications of the "NONOates". Free Radic Biol Med 2000;28:1463–9.
32. Lowe SW, Ruley HE, Jacks T, Housman DE. p53-dependent apoptosis modulates the cytotoxicity of anticancer agents. Cell 1993;74:957–67.
33. Bronfman M, Loyola G, Koenig CS. Isolation of intact organelles by differential centrifugation of digitonin-treated hepatocytes using a table Eppendorf centrifuge. Anal Biochem 1998;255:252–6.
34. Haupt Y, Maya R, Kazaz A, Oren M. Mdm2 promotes the rapid degradation of p53. Nature 1997;387:296–9.
35. Shieh SY, Ikeda M, Taya Y, Prives C. DNA damage-induced phosphorylation of p53 alleviates inhibition by MDM2. Cell 1997;91:325–34.
36. Zhang Y, Xiong Y. A p53 amino-terminal nuclear export signal inhibited by DNA damage-induced phosphorylation. Science 2001;292:1910–5.
37. Nakano K, Vousden KH. PUMA, a novel proapoptotic gene, is induced by p53. Mol Cell 2001;7:683–94.
38. Yu Y, Li CY, Little JB. Abrogation of p53 function by HPV16 E6 gene delays apoptosis and enhances mutagenesis but does not alter radiosensitivity in TK6 human lymphoblast cells. Oncogene 1997;14:1661–7.
39. van Engeland M, Nieland LJ, Ramaekers FC, Schutte B, Reutelingsperger CP. Annexin V-affinity assay: a review on an apoptosis detection system based on phosphatidylserine exposure. Cytometry 1998;31:1–9.
40. Sluss HK, Armata H, Gallant J, Jones SN. Phosphorylation of serine 18 regulates distinct p53 functions in mice. Mol Cell Biol 2004;24:976–84.
41. Burney S, Tamir S, Gal A, Tannenbaum SR. A mechanistic analysis of nitric oxide-induced cellular toxicity. Nitric Oxide 1997;1:130–44.
42. Brockhaus F, Brune B. p53 accumulation in apoptotic macrophages is an energy demanding process that precedes cytochrome *c* release in response to nitric oxide. Oncogene 1999;18:6403–10.
43. Little JB, Nagasawa H, Keng PC, Yu Y, Li CY. Absence of radiation-induced G_1 arrest in two closely related human lymphoblast cell lines that differ in p53 status. J Biol Chem 1995;270:11033–6.
44. Marchenko ND, Zaika A, Moll UM. Death signal-induced localization of p53 protein to mitochondria. A potential role in apoptotic signaling. J Biol Chem 2000;275:16202–12.
45. Chipuk JE, Kuwana T, Bouchier-Hayes L, et al. Direct activation of Bax by p53 mediates mitochondrial membrane permeabilization and apoptosis. Science 2004;303:1010–4.
46. Nakaya N, Lowe SW, Taya Y, Chenchik A, Enikolopov G. Specific pattern of p53 phosphorylation during nitric oxide-induced cell cycle arrest. Oncogene 2000;19:6369–75.
47. Yung HW, Bal-Price AK, Brown GC, Tolkovsky AM. Nitric oxide-induced cell death of cerebrocortical murine astrocytes is mediated through p53- and Bax-dependent pathways. J Neurochem 2004;89:812–21.
48. Rubbi CP, Milner J. Disruption of the nucleolus mediates stabilization of p53 in response to DNA damage and other stresses. EMBO J 2003;22:6068–77.